Published in final edited form as:
Mol Pharm. 2010 February 1; 7(1): 41. doi:10.1021/mp900153f.

Non-invasive evaluation of antiangiogenic effect in a mouse tumor model by DCE-MRI with Gd-DTPA cystamine copolymers

Xueming Wu[1], **Eun-Kee Jeong**[2], **Lyska Emerson**[3], **John Hoffman**[4], **Dennis L. Parker**[2], and **Zheng-Rong Lu**[1,5,*]

[1]Department of Pharmaceutics and Pharmaceutical Chemistry, Huntsman Cancer Institute, University of Utah, Salt Lake City, Utah 84108

[2]Department of Radiology, Huntsman Cancer Institute, University of Utah, Salt Lake City, Utah 84108

[3]Department of Pathology, Huntsman Cancer Institute, University of Utah, Salt Lake City, Utah 84108

[4]Molecular Imaging Program, Huntsman Cancer Institute, University of Utah, Salt Lake City, Utah 84108

[5]Department of Biomedical Engineering, Case Western Reserve University, Cleveland, OH 44106

Abstract

The efficacy of polydisulfide-based biodegradable macromolecular Gd(III) complexes, Gd-DTPA cystamine copolymers (GDCC), for assessing tumor microvascular characteristics and monitoring antiangiogenesis therapy was investigated in a mouse model using dynamic contrast-enhanced MRI (DCE-MRI). The mice bearing human colon tumor xenografts were intraperitoneally injected with an antiangiogenesis agent Avastin® three times in a week at a dose of 200 μg/mouse. DCE-MRI with GDCC of 40 KDa (GDCC-40) was performed before and at 36 hours after the first treatment with Avastin® and at the end of treatment (7 days). Gd(DTPA-BMA) was used as a low molecular weight control. The tumor vascular parameters, endothelial transfer coefficient K^{trans} and factional plasma volume f^{PV}, were calculated from the DCE-MRI data with a two-compartment model. The K^{trans} and f^{PV} in tumor periphery estimated by DCE-MRI with GDCC-40 before and after the antiangiogenesis treatment correlated well to tumor growth before and after the treatment in the tumor model. In contrast, the parameters estimated by Gd(DTPA-BMA) did not show significant correlation to the therapeutic efficacy. This study demonstrates that DCE-MRI with the biodegradable macromolecular MRI contrast agent can provide effective assessment of the antiangiogenic efficacy of Avastin® in the animal tumor model based on measured vascular parameters in tumor periphery.

Keywords

DCE-MRI; biodegradable macromolecular contrast agent; (Gd-DTPA) cystamine copolymers; antiangiogenic therapy; Avastin

Correspondence to: Dr. Zheng-Rong Lu, Department of Biomedical Engineering, Wickenden Building, Room 427, Case Western Reserve University, 10900 Euclid Avenue, Cleveland, OH 44106-7207, Phone: 216-368-0187, Fax: 216-368-4969, zxl125@case.edu.

Introduction

Angiogenesis, recruitment of neovasculature, is crucial for tumor growth and metastasis.[1–3] Several growth factors have been identified as possible regulators of angiogenesis.[1,4] One of most important regulators of angiogenesis is vascular endothelial growth factor (VEGF).5 Various inhibitors of VEGF have been developed to inhibit tumor growth by blocking tumor angiogenesis,6 including Avastin®, a humanized anti-VEGF monocolonal antibody.[7–11] Development of effective imaging technology for non-invasive assessment of the therapeutic efficacy of antiangiogenic agents is critical for the preclinical and clinical development of new effective anti-angiogenesis agents and for the clinical management of antiangiogenesis therapies. Dynamic contrast enhanced (DCE) MRI is a non-invasive imaging modality that can quantitatively measure tumor vascularity and tumor vascular parameters. DCE-MRI has been developed as a powerful tool for tumor characterization[12] and assessing early efficacy of anti-cancer therapies, including anti-angiogenesis therapy.13 Accurate and non-invasive evaluation of therapeutic efficacy is crucial to monitor and guide efficacious cancer treatment.

It has been shown that the size of MRI contrast agents is important for accurate characterization of tumor vascular parameters with DCE-MRI. Currently, most DCE-MRI studies are performed using low molecular contrast agents.[14] These agents rapidly diffuse from the vascular compartment to the interstitial space, resulting in overestimated tumor vascular parameters. They extravasate nonselectively through normal and lesion vasculature, which limits their ability to distinguish between normal and tumor tissues in DCE-MRI.[15] Macromolecular MRI contrast agents do not extravasate across the normal vasculature and can selectively penetrate tumor vasculature due to tumor vascular hyperpermeability. Several preclinical studies have shown that macromolecular MRI contrast agents are effective for quantitative characterization of tumor vascularity in DCE-MRI.[15,16] DCE-MRI with macromolecular contrast agents can effectively differentiate benign tumors from malignant tumors and accurately evaluate tumor response to anti-cancer treatment in animal models.[17–19] However, macromolecular agents are not approved for clinical applications because of their slow and incomplete elimination, which may result in toxic side effects due to long-term tissue retention of toxic Gd(III) ions in the body.[20]

Recently, we have developed a class of polydisulfide-based macromolecular Gd(III) complexes as biodegradable macromolecular MRI contrast agents to facilitate the excretion of Gd(III) chelates after the MRI examinations.[21–24] These agents initially behave as macromolecular agents for effective enhancement in tumor tissues, and then gradually degrade into low molecular weight Gd(III) complexes, which rapidly excrete from the body via renal glomerular filtration.[25–28] The biodegradable macromolecular MRI contrast agents have minimal tissue accumulation comparable to the clinical contrast agents. The biodegradable macromolecular contrast agents are also effective for quantitative characterization of tumor vascularity in DCE-MRI.29

In this study, we investigated the effectiveness of a biodegradable macromolecular MRI contrast agent, Gd-DTPA cystamine copolymers (GDCC), for assessing tumor microvascular changes in antiangiogenic treatment using an experimental human colon cancer model. A low molecular weight clinical contrast agent, Gd(DTPA-BMA) (MW = 574 Da), was used as a low molecular weight control. Tumor vascular parameters, K^{trans} and f^{PV}, were determined by DCE-MRI with both agents before and after the treatment with Avastin®. The tumor vascular parameters were evaluated in correlation to the tumor growth before and after the treatment.

Experimental Section

Animal models

The animal study was performed according to an animal study protocol approved by the Institutional Animal Care and Use Committee of the University of Utah. HT-29 human colon carcinoma cell line was purchased from American Type Culture Collection (ATCC, Manassas, VA). HT-29 cell line was cultured using ATCC complete growth medium (5 McCoy's Medium with 10% fetal bovine serum). Athymic female NCr-nu/nu nude mice (4–6 weeks old) were purchased from National Cancer Institute at Frederick, MD. The suspension of HT-29 cells in complete medium was mixed with Matrigel matrix (BD Biosciences, San Jose, CA) at 1:1 ratio. The mixtures (2×10^6 cells, 100 μl) were implanted subcutaneously in the flank of 12 mice when the mice were approximately 10–12 weeks old.

Contrast agents

Gd-DTPA cystamine copolymers (GDCC) were prepared as previously described[28]. The polymers were fractionated using a Superose 6 column on a Pharmacia FPLC system (Gaithersburg, MD) to prepare the contrast agent with narrow molecular weight distributions. The average molecular weights of the fractions were determined by size exclusion chromatography using poly[N-(2-hydroxypropyl)methacrylamide] as standard on an AKTA FPLC system (GE Biosciences, Piscataway, NJ). The fraction with a molecular weight of 40 KDa (GDCC-40) was used in this study. The Gd(III) content in the agents was determined by inductively coupled plasma optical emission spectroscopy (ICP-OES, Perkin Elmer Optima 3100XL). Gd(DTPA-BMA) (gadodiamide, MW: 574 Da) was obtained from GE Healthcare Inc., Princeton, NJ.

MRI

Mice were anesthetized by intraperitoneal injection of a mixture of Ketamine (Bedford, OH, 90 mg/kg) and Xylazine (St. Joseph, MO, 10 mg/kg). The mice were then placed with the tumors located approximately at the center of a coil. The anesthetized animals were placed on a heating pad before MRI and then wrapped in warm towels to maintain body temperature. A tail vein of mouse was catheterized with a 30 gauge needle connected with 2.5 m long tubing filled with heparinized saline. The contrast agents (100 μL) were pre-loaded into the tubing and manually injected within 3 seconds by flushing with 200 μL saline. The doses were 0.05 mmol-Gd/kg for GDCC-40 and 0.1 mmol-Gd/kg for Gd(DTPA-BMA). All images were acquired on a whole body clinical 3T MRI system (Tim-Trio, Siemens Medical Solutions, Erlangen, Germany) using a homemade quadrature transmit/receive saddle coil with 1.5 inch inner diameter and 3 inch length. A group of 6 mice with average weights of 23 g was used for each agent.

Three-dimensional MR images were acquired using a 3D turboFLASH sequence, followed by a 2D T_1-weighted spin-echo sequence before injection of the contrast agent. The 3D turboFLASH images were used to define the slice location for the 2D SE images. Dynamic MRI was performed to rapidly acquire 20 coronal slices with a 2D turboFLASH sequence for a period of 20 min with the temporal resolution of 6.0 seconds. After a delay of approximately 2 minutes of precontrast imaging, the contrast agents were administered into the tail vein via the catheter. Twenty 2D coronal SE images were then acquired for 20 minutes after the injection. Parameters of the 3D turboFLASH sequence were TR/TE = 7.40/2.60 ms, α= 25°, FOV = 52×120×24 mm^3 and matrix = 112×256×48 yielding 0.47×0.47×0.5 mm^3 spatial resolution. Imaging parameters for 2D SE sequence were TR/TE = 600/13 ms, α= 90°, FOV= 35×102 and acquisition matrix = 88×256 yielding 0.4×0.4 mm^2 inplane resolution with 0.8 mm slice thickness. The parameters of 2D turboFLASH sequence for DCE-MRI were TR/TE=5.80/2.10 ms, α=25°, FOV= 51×102 and acquisition matrix = 64×128 yielding 0.8×0.8

mm^2 inplane resolution with 0.8 mm thickness for total 20 slices that include a few slices covering the heart. Imaging time of each time frame was 6 seconds in DCE-MRI.

Evaluation of the Anti-angiogenic Efficacy of Avastin® with DCE-MRI

The DCE-MRI study and treatment with Avastin® were performed when the tumors reached approximately 1 cm in long diameter, about 3 weeks after tumor cells inoculation. A group of six mice each were used for DCE-MRI with GDCC-40 and the control agent Gd(DTPA-BMA). DCE-MRI experiment was performed before the treatment to determine the pretreatment values of tumor vascular parameters with both agents. Avastin® (Bevacizumab, Genentech, South San Francisco, CA) was then intraperitoneally injected at a dose of 200 μg/mouse every 2 days for 6 days starting on the day 22 of tumor implantation. DCE-MRI with both agents was performed at 36 hours and 7 days after the first injection of Avastin®. Tumor size was measured using a caliper during the study. Tumor volume was calculated using equation $V=AB^2/2$, where A is long diameter, B is short diameter.

Analysis of DCE-MRI Data

The 3D FLASH and 2D SE images were reconstructed and analyzed using Osirix software (http://homepage.mac.com/rossetantoine/osirix/). A package of programs based on MATLAB (The MathWorks, Inc., Natick, MA) was developed to process dynamic 2D FLASH data in DICOM format. Regions of interest (ROIs) were manually drawn at least six times at the right ventricle of the heart or tumor periphery for each image slice. The right ventricle of the heart was selected as ROI to obtain blood signal intensity (SI) or arterial input function. ROIs were limited to the tumor periphery for kinetic analysis because the tumor periphery is highly vascularized with angiogenic microvessels.[15] The tumor periphery was defined as the periphery zone of strong contrast enhancement. ROIs were also selected at the inner tumor tissues to study the changes of vascular parameters. The average signal intensity of the precontrast images (SI_0) in the ROIs was used as the pretreatment value. Signal enhancements after contrast injection were calculated as: $\Delta SI_t=(SI_t-SI_0)/SI_0$, where SI_t is the signal intensity within the ROIs at the time t post-contrast. It is assumed that ΔSI is proportional to the change of the contrast agent concentration, which is a reasonable approximation at low contrast agent concentration.[30]

The signal-time kinetic data were analyzed using a two-compartment bidirectional exchange kinetic model as shown in the equation 1[15],

$$C_T(t)=K^{trans}\int_0^t C_p(\theta)e^{-k_{ep}(t-\theta)}d\theta+f^{PV}C_p(t) \quad (1)$$

where $C_p(t)$ and $C_T(t)$ are the contrast agent concentrations in plasma and in the tumor, respectively. The concentration in blood, $C_B(t)$, were first converted to $C_p(t)$ by dividing by (1-Hct), where Hct is the hematocrit of mice. According to the literature[31], an average hematocrit value 0.42 was used in this study. K^{trans} is the endothelial transfer coefficient, k_{ep} the rate constant of reflux from the extravascular and extracellular space (EES) back to blood, θ a Laplace operator and f^{PV} the fractional plasma volume. The vascular parameters K^{trans} and f^{PV} in the tumor periphery were estimated by fitting the signal enhancement values of blood in the heart and tumor periphery using a nonlinear algorithm. Detailed pixel-by-pixel analysis was also performed in the tumor tissue to K^{trans} and f^{PV} maps in the tumor tissues.

Histologic Analysis

Mice were sacrificed at the end of the experiment and tumors were excised and fixed in 10 % formaldehyde solution for about 3 days. Then the tumor was cut in half along the midline of

tumor in the coronal plane corresponding to that used for the MR images and embedded in paraffin. From each of the two halves, six consecutive sections (5 μm thick) were sliced. One half was stained with conventional hematoxylin-eosin and the other half was stained with antibody to factor VIII. All sections were examined with microscopy. Tumor necrotic area, viable tumor cells and microvessel density were assessed and compared between the pre-treated and post-treated tumors.

Statistics Analysis

Statistical analysis was performed using a paired two-tailed Student's *t*-test (GraphPad Prism; GraphPad Software, San Diego, CA). A confidence interval of 95% ($p < 0.05$) was considered statistically significant. The tumor vascular parameters, K^{trans} and f^{PV}, were compared before and after the treatment.

Results

Figure 1 shows the tumor growth curve of the mice before and after the treatment with Avastin®. The HT-29 colon tumor xenografts grew rapidly and the average tumor volume reached about 508 ± 185 mm^3 3 weeks after inoculation (right before Avastin® treatment). Treatment was started on the day 22 by i.p. administration of Avastin® at a dose of 200 μg/mouse every 2 days in 6 days. The variation of tumor volume is relatively large due to different tumor size from different mice. The insert of figure 1 shows the normalized tumor growth percentage relative to the tumor size of day 20. Before treatment, tumor growth was significant ($p < 0.01$) when compared the tumor size of day 20 and 22. After the first treatment, tumor growth reduced with no significant difference ($p = 0.44$) when compared the tumor size of day 22 and 24. After the second and third treatment, tumor growth became significant again ($p < 0.05$). This result showed that tumor growth was temporarily arrested by the initial administration of Avastin® and then resumed after the second and third administrations at a slower rate.

Figure 2 shows the representative arterial input function and signal enhancement (ΔSI)–time curves in the tumor periphery for GDCC-40 and Gd(DTPA-BMA) before, and at 36 hours and 7 days after the first administration of Avastin®. The arterial input function showed that both agents have a high initial concentration after the injection. The low molecular weight Gd(DTPA-BMA) was then rapidly cleared from blood, while GDCC-40 was cleared at a relatively slow rate. At 36 hours after the first administration, the initial signal enhancement in tumor periphery with GDCC-40 decreased to approximately 50% of the baseline enhancement (pretreatment). The initial signal enhancement increased slightly at 7 days after three injections as compared to those measured at 36 hours after the first injection. However, the initial signal enhancement with Gd(DTPA-BMA) did not show significant changes of Gd(DTPA-BMA) uptake in tumor periphery before and after the treatment with Avastin®.

The vascular parameters K^{trans} and f^{PV} in the tumor periphery were calculated from the signal enhancement (ΔSI)–time data for each mouse before and after the treatment. Table 1 summarizes the average values of K^{trans} and f^{PV} in both tumor periphery and inner tumor tissue estimated from DCE-MRI with GDCC-40 and Gd(DTPA-BMA). Figure 3 plots the K^{trans} and f^{PV} parameters estimated from the agents before and after the treatments with Avastin®. Both K^{trans} and f^{PV} values in tumor periphery obtained from DCE-MRI with GDCC-40 significantly decreased at 36 hours after the first treatment as compared to the pretreatment values ($p < 0.05$). The values increased at 7 days after three treatments and were similar to the pretreatment values ($p > 0.05$). The average K^{trans} in the tumor core did not change significantly after the treatment as compared to the pretreatment values. The average f^{PV} in the tumor core after the treatment decreased significantly from the pretreatment values. In comparison, the K^{trans} and f^{PV} in both tumor periphery and tumor core estimated from DCE-MRI with Gd(DTPA-BMA) after

treatments were not significantly different from the pretreatment values ($p > 0.05$). The K^{trans} and f^{PV} values estimated from Gd(DTPA-BMA) were also much higher than those estimated from GDCC-40.

Figure 4 shows the representative color-coded K^{trans} and f^{PV} maps of tumor tissues constructed based on pixel-by-pixel analysis before and after the treatment with Avstin®. The maps revealed that tumor periphery had higher K^{trans} and f^{PV} values than the inner tumor tissues in all cases. The vascular parameters in the tumor periphery estimated from DCE-MRI with GDCC-40 were smaller than those estimated from Gd(DTPA-BMA). The number of pixels with high K^{trans} and f^{PV} values decreased after the treatment as shown in the maps from GDCC-40 as compared to those of pre-treatment. However, vascular parameter values in tumor periphery at 7 days after the treatment were higher than those at 36 hours after the first treatment (Figure 4A). The K^{trans} maps from DCE-MRI with Gd(DTPA-BMA) also revealed the reduction of pixel numbers of high K^{trans} values in the inner tumor tissue after the treatment, while the K^{trans} values in the tumor periphery remained high (Figure 4B). No significant difference was shown in the f^{PV} maps from Gd(DTPA-BMA) before and after the treatment.

Discussion

Antiangiogenic therapy is a new strategy for cancer treatment, which targets tumor vasculature and inhibits tumor angiogenesis. Several antiangiogenesis therapeutic agents have been approved by the FDA for cancer treatment[7–11]. More new agents are in various stages of preclinical and clinical development. Non-invasive imaging biomarkers can provide early and accurate evaluation of therapeutic efficacy of these agents, which is crucial for identification of suitable agents in preclinical drug development, and for patient management and efficacious cancer treatment in image-guided cancer therapy. In this study, we investigated the effectiveness of a biodegradable macromolecular MRI contrast agent, GDCC-40, for assessing tumor microvascular changes in antiangiogenic treatment with DCE-MRI in an animal tumor model. We have shown that DCE-MRI with GDCC-40 is effective for non-invasive and early evaluation of antiangiogenic therapy based on the estimated vascular parameters.

Avastin® is a humanized anti-VEGF-A antibody approved by the FDA to treat metastatic colorectal cancer, metastatic breast cancer and non-small cell lung cancer in combination with chemotherapies. It blocks tumor angiogenesis and inhibits tumor growth. The administration of Avastin® to mice bearing HT-29 human colon adenocarcinoma xenografts resulted in initial arrest of tumor growth after the first injection and then a relatively slow growth rate after further injections (Fig. 1). The mice body weight was also monitored at each time point of MRI scan (before, 36 h and 7 days after Avastin® therapy). Compared to the mice body weight at the first MRI scan (21.9 ± 1.3 g), there was no difference at the second (21.5 ± 1.2 g, p=0.43) or third (21.6 ± 1.8 g, p=0.68) MRI scan. This indicated that the mice health was not affected by the anesthesia or restraint during MRI scan, and the decreased tumor growth rate should be from the effect of Avastin® therapy.

The low therapeutic efficacy after the second and third administrations might be attributed to the fact that Avastin® neutralizes human VEGF-A[32–34] and might not be effective in neutralizing mouse VEGF-A and other forms of mouse VEGF. In this study, human tumor xenografts were implanted in mice and Avastin® might initially neutralize the human VEGF-A. A compensatory up-regulated murine VEGF released by the host might be responsible for the tumor angiogenesis and re-growth[35]. Furthermore, Avastin® could not neutralize other members of the VEGF gene family, including VEGF-B and VEGF-C, which may also play important roles in stimulating tumor angiogenesis and re-growth[1,2,33,36–38].

DCE-MRI with GDCC-40 was able to measure the changes of tumor vascular parameters, vascular permeability (K^{trans}) and fractional tumor plasma volume (f^{PV}), in correlation to therapeutic efficacy of Avastin® in the animal tumor model. Significant decrease of K^{trans} and f^{PV} was observed in viable tumor periphery with high angiogenesis at 36 hours after the first injection as compared to the pretreatment values ($p < 0.05$). The estimated K^{trans} and f^{PV} values then increased at 7 days after 3 administrations of Avastin® as tumor started re-growth, and became similar to the pretreatment values ($p > 0.05$). No significant changes were observed for the vascular parameters in tumor periphery estimated by DCE-MRI with Gd(DTPA-BMA) before and after the treatment with Avastin® ($p > 0.05$), because the agent non-selectively permeated through both normal and angiogenic blood vessels.

Macromolecular MRI contrast agents have been shown more effective than small molecular ones for characterization of tumor angiogenesis and evaluation of therapeutic efficacy of anti-angiogenesis therapies[18,19,39,40]. However, clinical development of macromolecular contrast agents is limited by their slow excretion and consequent potential toxic side effects. Biodegradable macromolecular agents based on polydisulfide Gd(III) chelates have been developed to facilitate the excretion after the MRI studies. Due to their degradability in plasma, these agents have relatively short blood half-lives as compared to the non-degradable macromolecular contrast agents. However, the degradation of GDCC was relatively slow in the first 20 minutes in the incubation with fresh rat plasma[28,41], which was the duration of DCE-MRI experiment of this study. The biodegradable macromolecular contrast agent still behaved as a macromolecular contrast agent in the initial period of DCE-MRI study for effective evaluation of therapeutic efficacy[42]. Our previous studies has shown that the vascular parameters estimated by DCE-MRI with the biodegradable macromolecular contrast agents was slightly higher than those estimated with albumin-(Gd-DTPA), but lower than those estimated with a low molecular weight clinical contrast agent[29]. This study has shown that the biodegradable macromolecular contrast agent GDCC-40 was able to provide early assessment of the tumor response to antiangiogenic therapy in DCE-MRI based on estimated vascular parameters. Since GDCC-40 initially behaved as a macromolecular contrast agent, it was able to effectively estimate the changes in tumor vascular permeability to macromolecules in DCE-MRI, particularly in highly angiogenic tumor periphery.

This is the first attempt to evaluate the potential of the biodegradable macromolecular contrast agents in early assessment of tumor response to antiangiogensis therapy. This study had several limitations. The DCE-MRI sequence we used was not able to accurately measure the kinetic changes of the concentrations of contrast agents. Our previous studies showed that the relaxivities of the biodegradable macromolecular contrast agent GDCC did not vary substantially with different molecular weights. Therefore, the relaxivities of GDCC were considered constant during the period of experiment. In this study, we did not observe any significant changes in tumor microvessel density before and after the treatment with Avastin® in histological studies. The histological data did not correlate to the tumor vascular parameters estimated with DCE-MRI and GDCC-40 and the tumor growth curve. Further and more broadly designed studies covering various preclinical and clinical conditions are required to validate the effectiveness of the biodegradable contrast agent in the early assessment of tumor response to cancer therapies.

In conclusion, the biodegradable macromolecular contrast agent, GDCC-40, was effective to estimate the changes of the tumor vascular parameters before and after the treatment with antiangiogenic therapeutics in DCE-MRI. DCE-MRI with GDCC-40 has a potential to non-invasively assess early tumor response to antiangiogenic therapy and to follow the therapeutic efficacy in the treatment.

Acknowledgments

The authors thank Dr. Yong-En Sun for the animal handling, Dr. James Lee for technical assistance in MRI data acquisition, and Oliver Jeong for making the quadrature transmit/receive saddle coil. This work was supported in part by the NIH grant R01 EB00489.

References

1. Masabumi, Shibuya. Signal transduction of VEGF receptors toward angiogenesis. In: Napoleone Ferrara CRC Press Taylor & Frabcus Grup Boca Raton Londo New York. , editor. Angiogenesis From Basic Science to Clinical Applications. 2007. p. 37-51.
2. Yancopoulos GD, Davis S, Gale NW, Rudge JS, Wiegand SJ, Holash J. Vascular-specific growth factors and blood vessel formation. Nature 2000;407:242–248. [PubMed: 11001067]
3. Ferrara N. VEGF and the quest for tumour angiogenesis factors. Nat. Rev. Cancer 2002;2:795–803. [PubMed: 12360282]
4. Klagsbrun M, D'Amore PA. Regulators of angiogenesis. Annu. Rev. Physiol 1991;53:217–239. [PubMed: 1710435]
5. Ferrara N. Vascular endothelial growth factor: basic science and clinical progress. Endocr. Rev 2004;25:581–611. [PubMed: 15294883]
6. Cristofanilli M, Charnsangavej C, Hortobagyi GN. Angiogenesis modulation in cancer research: novel clinical approaches. Nat. Rev. Drug Discov 2002;1:415–426. [PubMed: 12119743]
7. Duda DG, Batchelor TT, Willett CG, Jain RK. VEGF-targeted cancer therapy trategies: current progress, hurdles and future prospects. Trends Mol. Med 2007;13:223–230. [PubMed: 17462954]
8. Midgley R, Kerr D. Bevacizumab-current status and future directions. Ann. Oncol 2005;16:999–1004. [PubMed: 15939715]
9. Ferrara N, Hillan KJ, Novotny W. Bevacizumab (Avastin), a humanized anti-VEGF monoclonal antibody for cancer therapy. Biochem. Biophys. Res. Commun 2005;333:328–335. [PubMed: 15961063]
10. Shih T, Lindley C. Bevacizumab: an angiogenesis inhibitor for the treatment of solid malignancies. Clin. Ther 2006;28:1779–1802. [PubMed: 17212999]
11. Krämer I, Lipp HP. Bevacizumab, a humanized antiangiogenic monoclonal antibody for the treatment of colorectal cancer. J. Clin. Pharm. Ther 2007;32:1–14. [PubMed: 17286784]
12. Tuncbilek N, Karakas HM, Okten OO. Dynamic contrast enhanced MRI in the differential diagnosis of soft tissue tumors. Eur. J. Radiol 2005;53:500–505. [PubMed: 15741025]
13. Marzola P, Degrassi A, Calderan L, Farace P, Nicolato E, Crescimanno C, Sandri M, Giusti A, Pesenti E, Terron A, Sbarbati A, Osculati F. Early antiangiogenic activity of U11248 evaluated in vivo by dynamic contrast-enhanced magnetic resonance imaging in an experimental model of colon carcinoma. Clin. Cancer Res 2005;11:5827–5832. [PubMed: 16115922]
14. Thoeny HC, De Keyzer F, Vandecaveye V, Chen F, Sun X, Bosmans H, Hermans R, Verbeken EK, Boesch C, Marchal G, Landuyt W, Ni Y. Effect of vascular targeting agent in rat tumor model: dynamic contrast-enhanced versus diffusion-weighted MR imaging. Radiology 2005;237:492–499. [PubMed: 16192323]
15. Daldrup H, Shames DM, Wendland M, Okuhata Y, Link PM, Rosenau W, Lu Y, Brasch RC. Correlation of dynamic contrast-enhanced MR imaging with histologic tumor grade: comparison of macromolecular and small-molecular contrast media. American Journal of Roentgenology 1998;171:941–949. [PubMed: 9762973]
16. de Lussanet QG, Langereis S, Beets-Tan RG, et al. Dynamic contrast-enhanced MR imaging kinetic parameters and molecular weight of dendritic contrast agents in tumor angiogenesis in mice. Radiology 2005;235:65–72. [PubMed: 15731376]
17. Fan X, Medved M, River JN, Zamora M, Corot C, Robert P, Bourrinet P, Lipton M, Culp RM, Karczmar GS. New model for analysis of dynamic contrast-enhanced MRI data distinguishes metastatic from nonmetastatic transplanted rodent prostate tumors. Magn. Reson. Med 2004;51:487–494. [PubMed: 15004789]

18. Bhujwalla ZM, Artemov D, Natarajan K, Solaiyappan M, Kollars P, Kristjansen PE. Reduction of vascular and permeable regions in solid tumors detected by macromolecular contras magnetic resonance imaging after treatment with antiangiogenic agent TNP-470. Clin. Cancer Res 2003;9:355–362. [PubMed: 12538488]
19. Marzola P, Degrassi A, Calderan L, Farace P, Nicolato E, Crescimanno C, Sandri M, Giusti A, Pesenti E, Terron A, Sbarbati A, Osculati F. Early antiangiogenic activity of SU11248 evaluated in vivo by dynamic contrast-enhanced magnetic resonance imaging in an experimental model of colon carcinoma. Clin. Cancer Res 2005;11:5827–5832. [PubMed: 16115922]
20. Schmiedl U, Ogan M, Paajanen H, Marotti M, Crooks L, Brito A, Brasch R. Albumin labeled with Gd-DTPA as an intravascular, blood pool-enhancing agent for MRI: biodistribution and imaging studies. Radiology 1987;162:205–210. [PubMed: 3786763]
21. Lu Z-R, Mohs AM, Zong Y, Feng Y. Polydisulfide Gd(III) chelates as biodegradable macromolecular magnetic resonance imaging contrast agents. Intl. J. Nanomed 2006;1:31–40.
22. Zong Y, Wang X, Goodrich KC, Mohs AM, Parker DL, Lu ZR. Contrast-enhanced MRI with new biodegradable macromolecular Gd(III) complexes in tumor-bearing mice. Magn. Reson. Med 2005;53:835–842. [PubMed: 15799038]
23. Zong Y, Ke T, Mohs AM, Guo J, Parker DL, Lu Z-R. Effect of size and charge on in vivo MRI contrast enhancement of polydisulfide Gd(III) complexes. J. Controlled Rel 2006;112:350–356.
24. Kaneshiro T, Ke T, Jeong EK, Parker DL, Lu Z-R. (Gd-DTPA)-(L-cystine bisalkylamide) copolymers as novel biodegradable macromolecular contrast agents for MR blood pool imaging. Pharm. Res 2006;23:1285–1294. [PubMed: 16729223]
25. Wang X, Feng Y, Ke T, Schabel M, Lu Z-R. Pharmacokinetics and tissue retention of (Gd-DTPA)-cystamine copolymers, a biodegradable macromolecular magnetic resonance imaging contrast agent. Pharm. Res 2005;22:596–602. [PubMed: 15846467]
26. Feng Y, Zong Y, Ke T, Jeong EK, Parker DL, Lu Z-R. Pharmacokinetics, biodistribution and contrast enhanced MR blood pool imaging of Gd-DTPA cystine copolymers and Gd-DTPA cystine diethyl ester copolymers in a rat model. Pharm. Res 2006;23:1736–1742. [PubMed: 16850267]
27. Mohs A, Nguyen T, Jeong EK, Feng Y, Emerson L, Zong Y, Parker DL, Lu Z-R. Modification of Gd-DTPA cystine copolymers with PEG-1000 optimizes pharmacokinetics and tissue retention for magnetic resonance angiography. Magn. Reson. Med 2007;58:110–118. [PubMed: 17659618]
28. Lu Z-R, Parker DL, Goodrich KC, Wang X, Dalle JG, Buswell HR. Extracellular biodegradable macromolecular gadolinium(III) complexes for MRI. Magn. Reson. Med 2004;51:27–34. [PubMed: 14705042]
29. Feng Y, Jeong E-K, Mohs A, Emerson L, Lu Z-R. Characterization of tumor angiogenesis with dynamic contrast enhanced magnetic resonance imaging and biodegradable macromolecular contrast agents in mice. Magn. Reson. Med 2008;60:1347–1352. [PubMed: 19025902]
30. Shames DM, Kuwatsuru R, Vexler V, Muhler A, Brasch RC. Measurement of capillary permeability to macromolecules by dynamic magnetic resonance imaging: a quantitative noninvasive technique. Magn. Reson. Med 1993;29:616–622. [PubMed: 8505897]
31. Trune DR, Kempton JB, Gross ND. Mineralocorticoid receptor mediates glucocorticoid treatment effects in the autoimmune mouse ear. Hear Res 2006;212:22–32. [PubMed: 16307853]
32. Presta LG, Chen H, O'Connor SJ, Chisholm V, Meng YG, Krummen L, Winkler M, Ferrara N. Humanization of an anti-vascular endothelial growth factor monoclonal antibody for the therapy of solid tumors and other disorders. Cancer Res 1997;57:4593–4599. [PubMed: 9377574]
33. Ferrara N, Hillan KJ, Novotny W. Bevacizumab (Avastin), a humanized anti-VEGF monoclonal antibody for cancer therapy. Biochem. Biophys. Res. Commun 2005;333:328–335. [PubMed: 15961063]
34. Ferrara N, Hillan KJ, Gerber HP, Novotny W. Discovery and development of bevacizumab, an anti-VEGF antibody for treating cancer. Nat. Rev. Drug Discov 2004;3:391–400. [PubMed: 15136787]
35. Gerber HP, Kowalski J, Sherman D, Eberhard DA, Ferrara N. Complete inhibition of rhabdomyosarcoma xenograft growth and neovascularization requires blockade of both tumor and host vascular endothelial growth factor. Cancer Res 2000;60:6253–6258. [PubMed: 11103779]

36. Stoeltzing O, Liu W, Reinmuth N, Parikh A, Ahmad SA, Jung YD, Fan F, Ellis LM. Angiogenesis and antiangiogenic therapy of colon cancer liver metastasis. Ann. Surg. Oncol 2003;10:722–733. [PubMed: 12900362]

37. Bruns CJ, Solorzano CC, Harbison MT, Ozawa S, Tsan R, Fan D, Abbruzzese J, Traxler P, Buchdunger E, Radinsky R, Fidler IJ. Blockade of the epidermal growth factor receptor signaling by a novel tyrosine kinase inhibitor leads to apoptosis of endothelial cells and therapy of human pancreatic carcinoma. Cancer Res 2000;60:2926–2935. [PubMed: 10850439]

38. Yuan F, Chen Y, Dellian M, Safabakhsh N, Ferrara N, Jain RK. Time-dependent vascular regression and permeability changes in established human tumor xenografts induced by an anti-vascular endothelial growth factor/vascular permeability factor antibody. Proc. Natl. Acad. Sci. USA 1996;93:14765–14770. [PubMed: 8962129]

39. Jordan BF, Runquist M, Raghunand N, Baker A, Williams R, Kirkpatrick L, Powis G, Gillies RJ. Dynamic contrast-enhanced and diffusion MRI show rapid and dramatic changes in tumor microenvironment in response to inhibition of HIF-1 alpha using PX-478. Neoplasia 2005;7:475–485. [PubMed: 15967100]

40. Vogel-Claussen J, Gimi B, Artemov D, Bhujwalla ZM. Diffusion-weighted and macromolecular contrast enhanced MRI of tumor response to antivascular therapy with ZD6126. Cancer Biol Ther 2007;6:1469–1475. [PubMed: 17881899]

41. Zong Y, Wang X, Jeong EK, Parker DL, Lu Z-R. Structural effect on degradability and in vivo contrast enhancement of polydisulfide Gd(III) complexes as biodegradable macromolecular contrast agents. Magn. Reson. Imaging 2009;27:503–511. [PubMed: 18814987]

42. Feng Y, Emerson L, Jeong EK, Parker DL, Lu ZR. Non-invasive assessment of the efficacy of indocyanine green enhanced photothermal cancer therapy with dynamic contrast enhanced MRI using a biodegradable macromolecular contrast agent. J. Magn. Reson. Imaging 2009;27:401–406. [PubMed: 19629979]

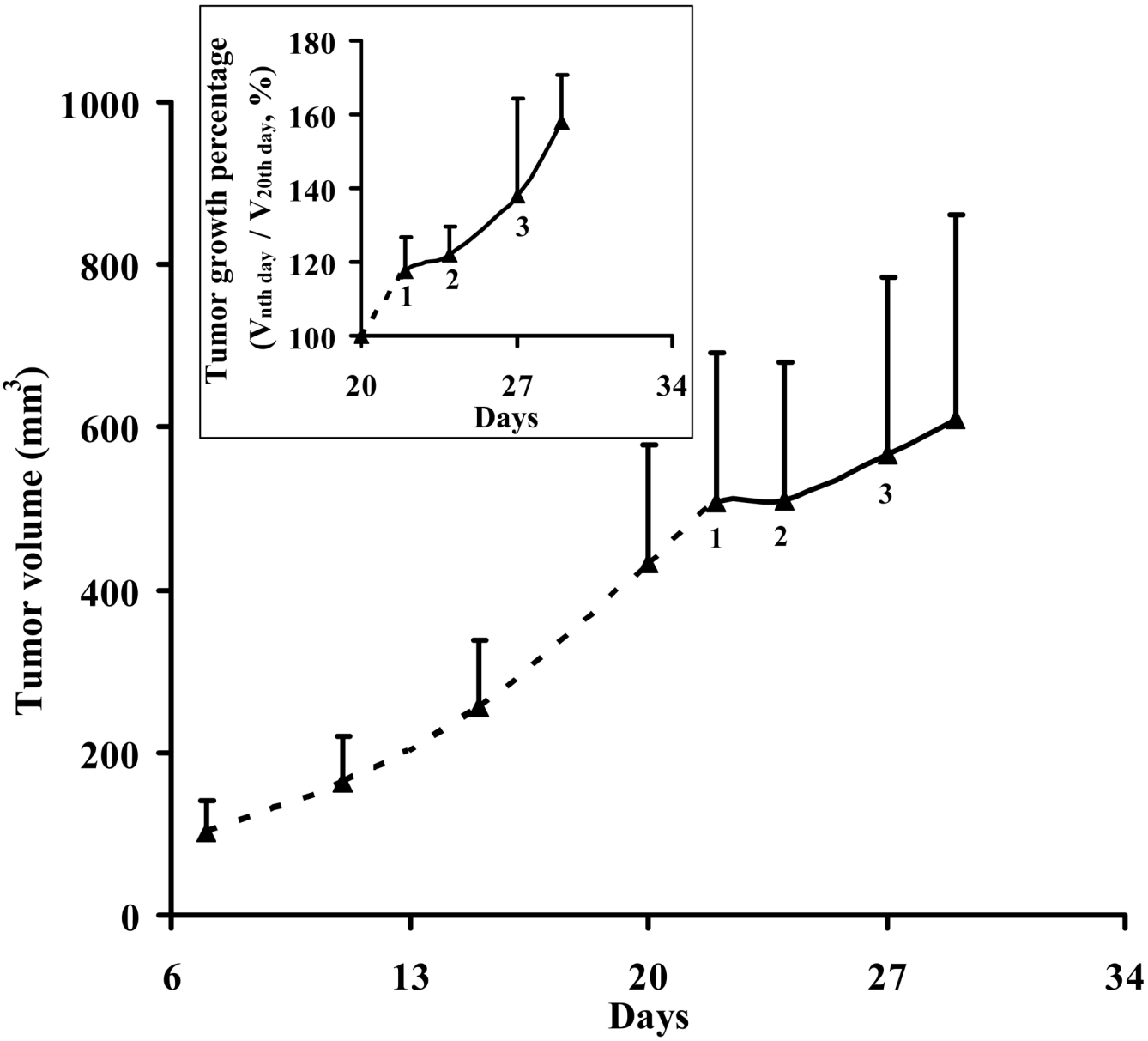

Figure 1.

Tumor volume and normalized tumor growth percentage relative to the tumor size of day 20 (Inserted figure) before and after treatment with Avastin®. Treatment was started on the day 22 by i.p. administration of Avastin® at a dose of 200 μg/mouse every 2 days in 6 days. 1: First treatment; 2: Second treatment; 3: Third treatment. Tumor growth was temporarily arrested by initial administration of Avastin® and then resumed at a slower rate even after the second and third administrations.

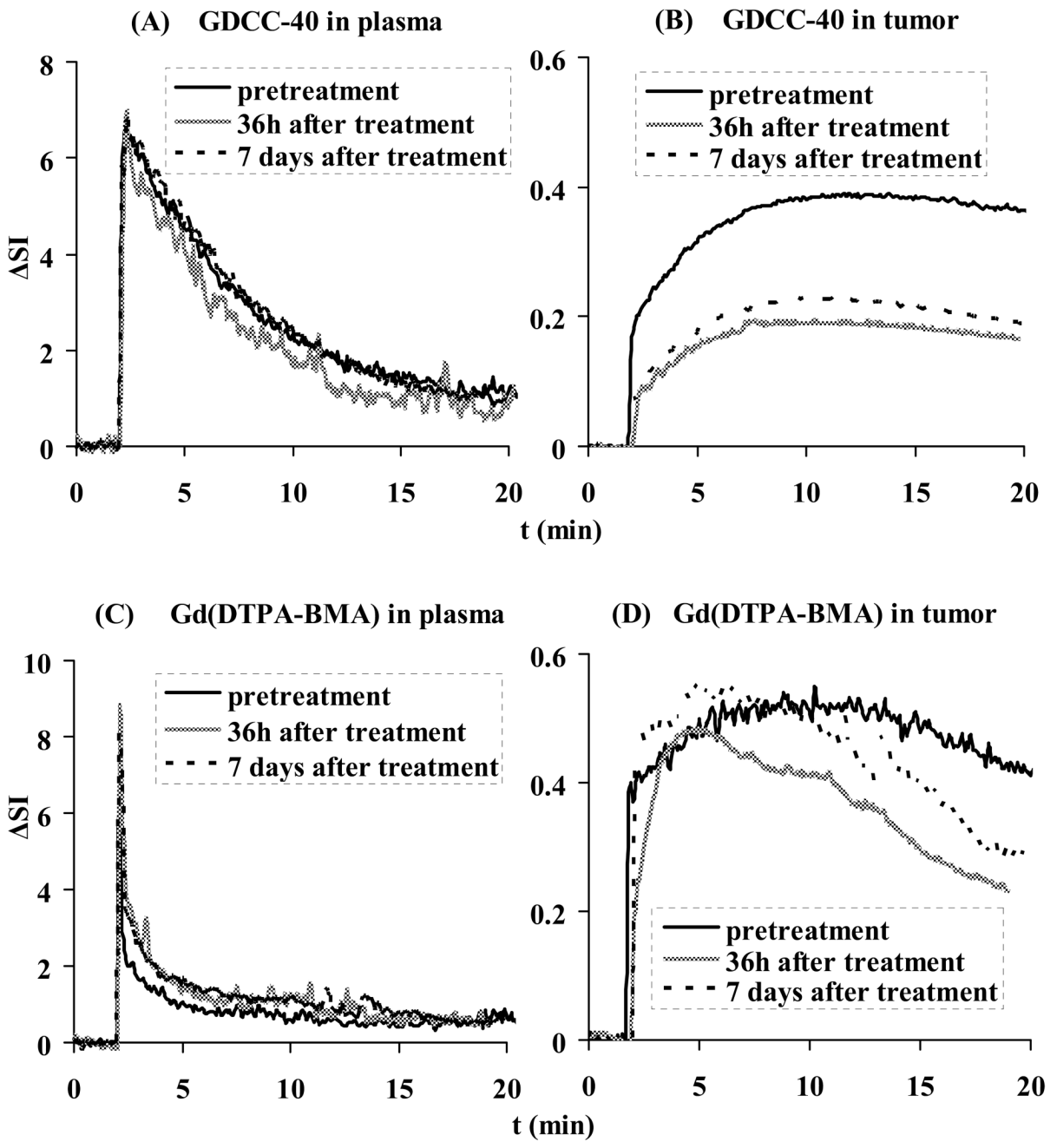

Figure 2.
Representative contrast enhancement-time curves in plasma and tumor for GDCC-40 (A, B) and Gd(DTPA-BMA) (C, D) before, 36 h and 7 days after the first administration of Avastin®.

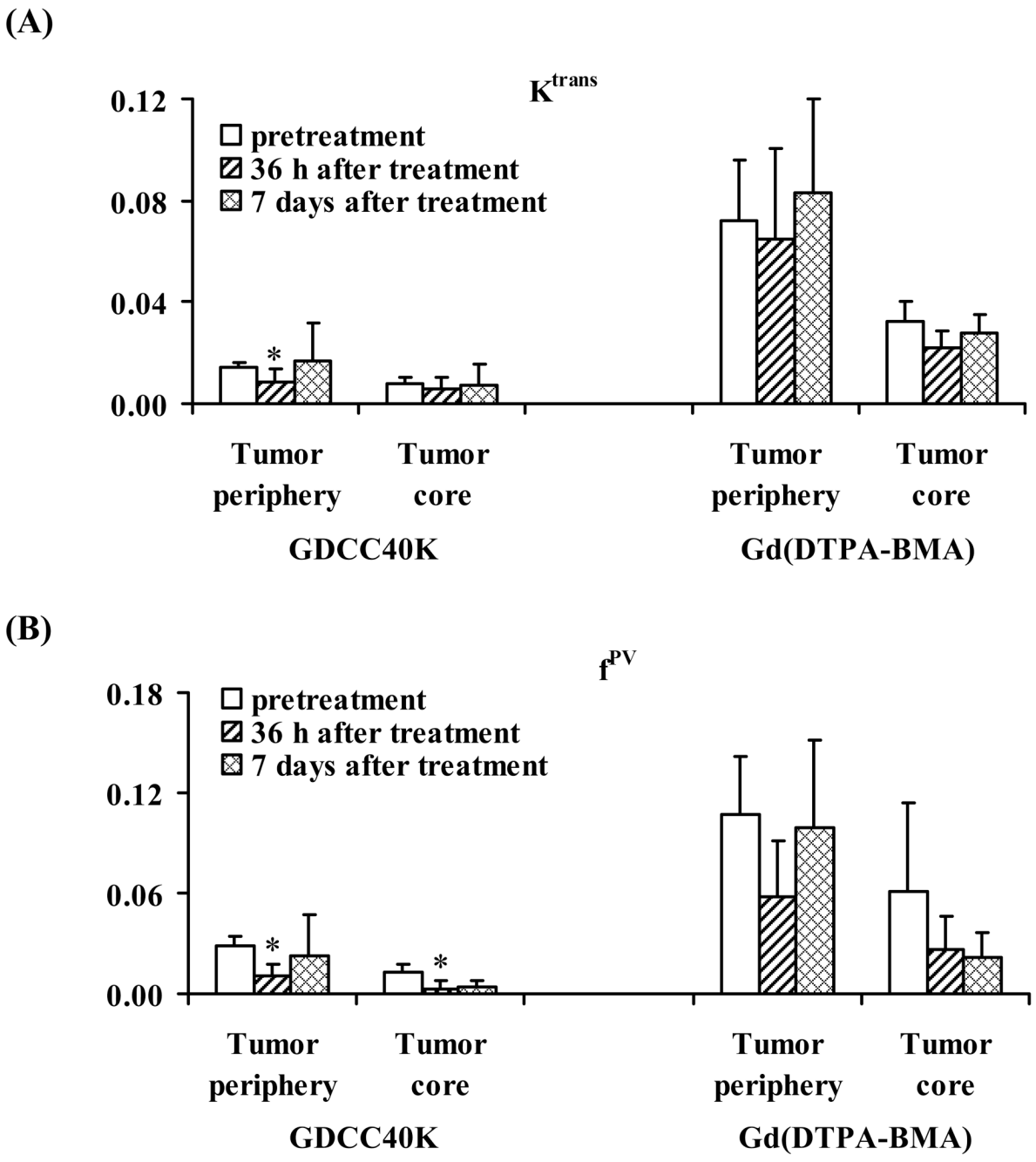

Figure 3.

Graphs showing change in K^{trans} (A) and f^{PV} (B) for GDCC-40 and Gd(DTPA-BMA) before and after Avastin administration. *: $P<0.05$. K^{trans} = endothelial transfer coefficient (mL of plasma/mL of tissue/min), f^{PV} = fractional vascular volume (mL of plasma/ mL of tissue).

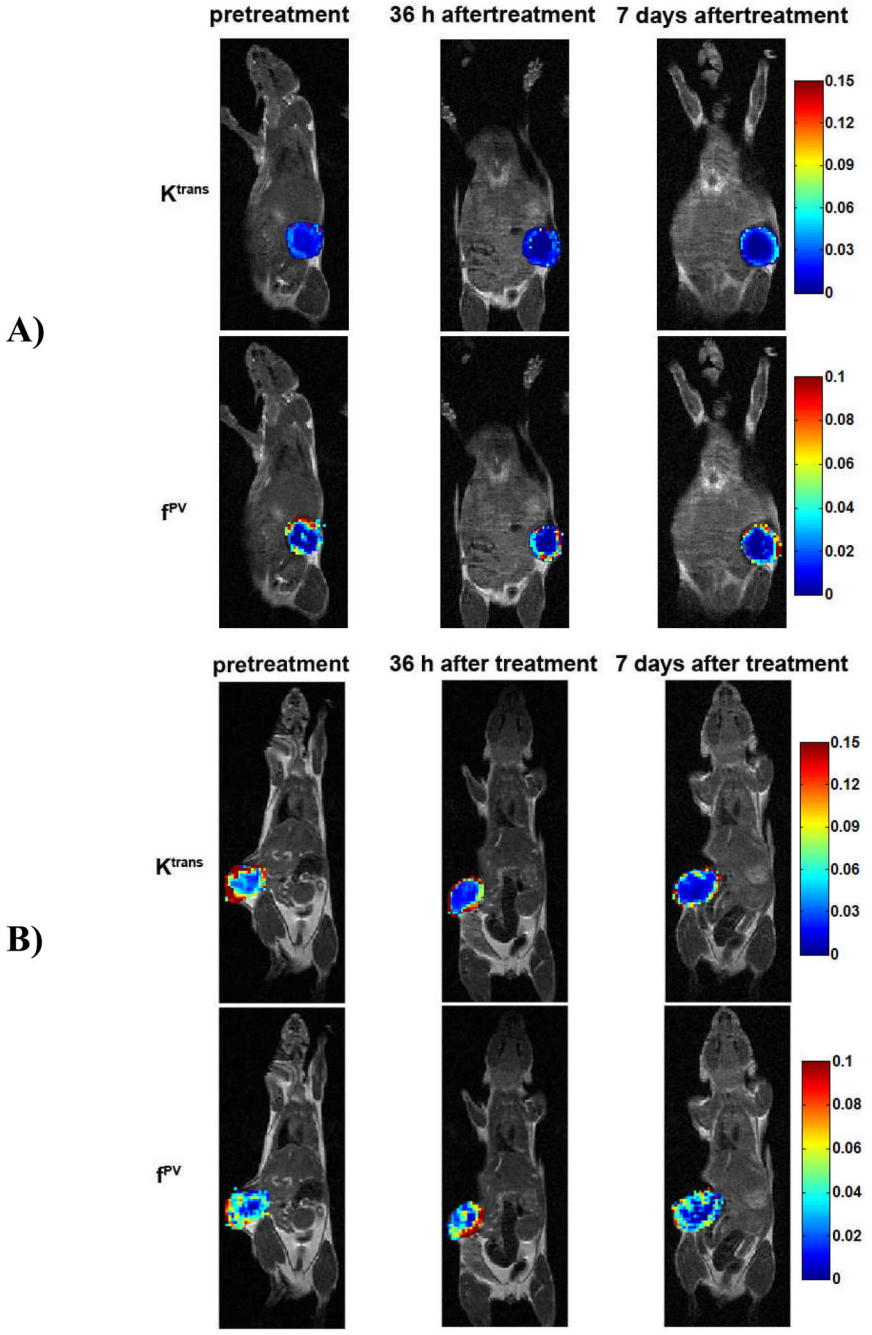

Figure 4.

Representative color-coded maps of K^{trans} and f^{PV} values measured for the voxels in the central section through the tumor. A is from the tumor of GDCC-40 injection group and B is from the tumor of Gd(DTPA-BMA) injection group.

Table 1

Tumor vascular parameters determined by DCE-MRI before and after administration of Avastin®

	GDCC-40			Gd(DTPA-BMA)		
	Pre	**Post 36 h**	**Post 7 days**	**Pre**	**Post 36 h**	**Post 7 days**
			K^{trans} (mL of plasma/mL of tissue/min)			
Tumor periphery	0.014 ± 0.002	0.009 ± 0.005*	0.017 ± 0.014	0.072 ± 0.024	0.065 ± 0.036	0.083 ± 0.038
Tumor core	0.008 ± 0.003	0.006 ± 0.005	0.007 ± 0.009	0.032 ± 0.008	0.022 ± 0.007	0.028 ± 0.007
			f^{PV} (mL of plasma/ mL of tissue)			
Tumor periphery	0.029 ± 0.006	0.011 ± 0.007*	0.023 ± 0.025	0.109 ± 0.035	0.058 ± 0.033	0.100 ± 0.052
Tumor core	0.013 ± 0.005	0.003 ± 0.005*	0.004 ± 0.003	0.061 ± 0.053	0.027 ± 0.020	0.022 ± 0.015

*Statistically significant from pretreatment values ($p<0.05$)